Magnetoresistance of a (γ- Fe 2 O 3) 80 Ag 20 nanocomposite prepared in reverse micelles

Joan A. Wiemann, Everett E. Carpenter, Jason Wiggins, Weilie Zhou, Jinke Tang, Sichu Li, Vijay T. John, Gary J. Long, and Amitabh Mohan

Citation: Journal of Applied Physics **87**, 7001 (2000); doi: 10.1063/1.372911
View online: http://dx.doi.org/10.1063/1.372911
View Table of Contents: http://scitation.aip.org/content/aip/journal/jap/87/9?ver=pdfcov
Published by the AIP Publishing

Novel Nanoscale Structures J. A. C. Bland, Chairman

Magnetoresistance of a $(\gamma\text{-}Fe_2O_3)_{80}Ag_{20}$ nanocomposite prepared in reverse micelles

Joan A. Wiemann
Department of Physics and Advanced Materials Research Institute, University of New Orleans, New Orleans, Louisiana 70148

Everett E. Carpenter, Jason Wiggins, and Weilie Zhou
Advanced Materials Research Institute, University of New Orleans, New Orleans, Louisiana 70148

Jinke Tang
Department of Physics and Advanced Materials Research Institute, University of New Orleans, New Orleans, Louisiana 70148

Sichu Li and Vijay T. John
Department of Chemical Engineering, Tulane University, New Orleans, Louisiana 70118-5698

Gary J. Long and Amitabh Mohan
Department of Chemistry, University of Missouri-Rolla, Rolla, Missouri 65409-0010

The magnetic and transport properties of a $(\gamma\text{-}Fe_2O_3)_{80}Ag_{20}$ nanocomposite, prepared by a reverse micelle technique, have been studied. $\gamma\text{-}Fe_2O_3$ nanoparticles and Ag particles were individually synthesized in reverse micelles. The nanocomposite material was then prepared by mixing the two different particles in a $\gamma\text{-}Fe_2O_3$/Ag molar ratio 80/20. The morphology of the nanoparticles was examined with transmission electron microscopy. Mössbauer spectra revealed no obvious presence of any divalent iron. Zero field cooled and field cooled magnetic susceptibilities indicated a blocking temperature of about 40 K. Negative magnetoresistance was observed resembling that in ball milled $\gamma\text{-}Fe_2O_3$/Ag nanocomposites. However, the magnitude of the negative magnetoresistance is smaller and is ~2.2% at 220 K and 9 T. Two possible mechanisms, spin-dependent hopping and tunneling across magnetic barriers, are discussed.
[S0021-8979(00)47208-7]

There are many studies of the magnetic properties of the technologically important nanophase iron oxide particles. The properties of these nanophase particles can be quite different from the bulk form of the oxides and by forming nanocomposites the electrical or magnetic properties of the nanophase oxides may be tailored or enhanced beyond those of the single-phase materials. Because of its chemical stability and low cost, maghemite, $\gamma\text{-}Fe_2O_3$ is often used in the manufacture of magnetic pigments for electronic recording media and in the production of ferrofluids.[1] The subject of this article is a new nanocomposite, $(\gamma\text{-}Fe_2O_3)_{80}(Ag)_{20}$, prepared in reverse micelles.

In a related work, $(\gamma\text{-}Fe_2O_3)_{100-x}(Ag)_x$, nanocomposites were produced using mechanical milling.[2] X-ray diffraction (XRD) analysis of the mechanically milled nanocomposites indicates that the average crystallite size of the $\gamma\text{-}Fe_2O_3$ is ~20 nm and Mössbauer spectroscopy indicates that ~3.7% of the iron is in the Fe^{2+} state. The presence of the impurity phase is a direct result of prolonged ball milling. Magnetoresistance (MR) was determined to be ~10% at 180 K and 9 T. The negative MR is believed to arise from the field dependent electron hopping between Fe^{2+} and Fe^{3+} ions.[2] In this article, the magnetoresistive properties of the reverse micelles nanocomposite are discussed and compared with the ball-milled composites.

The $\gamma\text{-}Fe_2O_3$/Ag nanocomposite was prepared from particles synthesized in reverse micelles $\gamma\text{-}Fe_2O_3$ and Ag nanoparticles were individually synthesized in reverse micelles using sodium dioctylsulfosuccinate (AOT) as the surfactant, isooctane as the oil phase, and aqueous reactants as the water phase. Reactants for $\gamma\text{-}Fe_2O_3$ were $FeSO_4$ and NH_4OH, and for Ag the reactants were $AgNO_3$ and hydrazine. After drying, the $\gamma\text{-}Fe_2O_3$/Ag granular nanocomposite was prepared by mixing the two different particles in an isooctane solution at a $\gamma\text{-}Fe_2O_3$/Ag molar ratio of 80/20. After the mixed particles were dried the surfactant was removed. Transmission electron microscopy (TEM) indicates that, before mixing and forming pellets at 15 kps, both the individual particles are spherical. Figure 1 shows that the random distribution and the variable sizes of the particles in the $(\gamma\text{-}Fe_2O_3)_{80}Ag_{20}$ composite pressed pellet. The typical particle size is 10 nm for $\gamma\text{-}Fe_2O_3$ and 20 nm for Ag.

X-ray diffraction analysis was performed on the nanocomposite using a Philips X'pert Powder Diffractometer. Average crystallite sizes were estimated using the Scherrer equation. The $\gamma\text{-}Fe_2O_3$ crystallite size is ~8 mm. The Ag crystallites are ~25 nm if variations due to strain are ig-

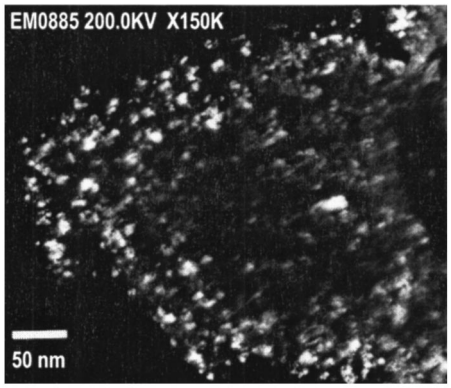

FIG. 1. TEM micrograph of a section of a pressed pellet of $(\gamma\text{-}Fe_2O_3)_{80}Ag_{20}$. Bright images are Ag particles, lighter images are aggregated $\gamma\text{-}Fe_2O_3$ particles.

nored. XRD indicates that the material has two distinguishable phases and is free of any impurity within the XRD detection limits. Synthetic $\gamma\text{-}Fe_2O_3$ has a tetragonal crystal structure indicative of the formation of a superlattice structure resulting from cation and vacancy ordering. The extent of the vacancy ordering is reduced when the crystallite size of the precursor is <200 nm.[1] Because the reverse micelles confined the reactants to crystallite sizes <10 nm, it is assumed that ordering of the vacancies in the spinel structure may be prohibited, thus producing a pattern with no characteristic superstructure lines. With the increase in crystallographic symmetry from tetragonal to cubic, the resultant XRD pattern is nearly indistinguishable from that of the spinel, Fe_3O_4, the difference being a slight shift in peak position. Therefore, to determine the presence of an impurity phase containing iron in the Fe^{2+} state, Mössbauer spectral studies were performed.

The Mössbauer spectra were measured at 295 and 78 K on a constant-acceleration spectrometer, which utilized a room temperature rhodium matrix cobalt-57 source and was calibrated at room temperature with α-iron foil. All isomer shifts are given relative to room temperature α-iron foil. The 295 K spectrum, see Fig. 2(a), indicates that the silver supported $\gamma\text{-}Fe_2O_3$ particles are superparamagnetic (SP) at 295 K as would be expected for fine particles. The 295 K spectrum has been fit with a distribution of symmetric quadrupole doublets and both the resulting average isomer shift of 0.354 mm/s and average quadrupole splitting of 0.68 mm/s are characteristic of fine $\gamma\text{-}Fe_2O_3$ particles. It is of interest to point out that the sample contains at most traces of divalent iron. The very weak absorption at $\sim$2.5 mm/s may result from the presence of some divalent iron. However, fits of this component indicate that, at most, only one percent of the iron is present as Fe^{2+}. The 78 K spectrum, see Fig. 2(b), clearly indicates that the SP $\gamma\text{-}Fe_2O_3$ particles are beginning to show the onset of slow magnetic relaxation on the Mössbauer time scale of 10^{-8} s. This is typical of fine SP $\gamma\text{-}Fe_2O_3$ particles whose blocking temperature, T_b, is $\sim$40 K, see below. As a consequence, the 78 K spectrum has been fit with a combination of a relaxation broadened magnetic sextet and a SP doublet, see Fig. 2(b). The resulting average isomer shift of 0.49 mm/s and hyperfine field of 58 kOe are typical of SP $\gamma\text{-}Fe_2O_3$ particles with a T_b of 40 K. At 78 K

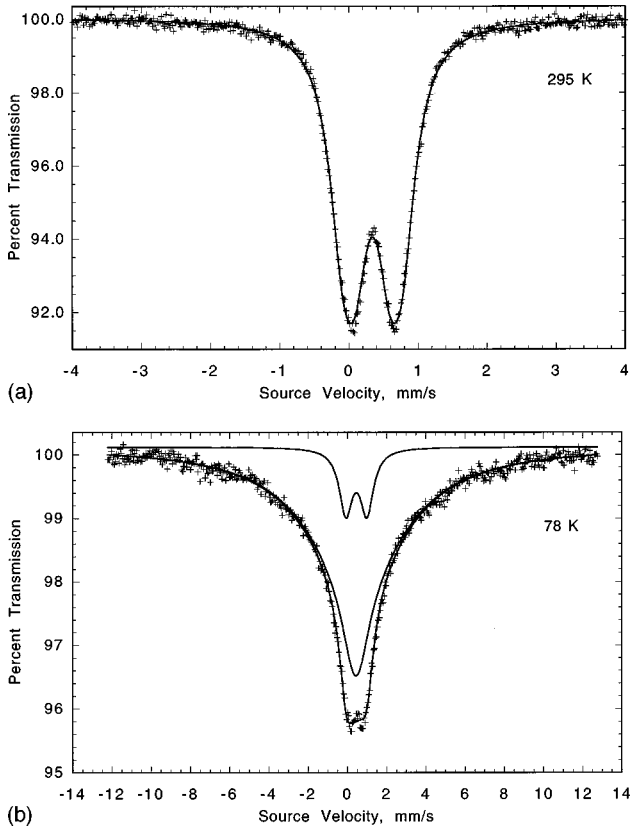

FIG. 2. The iron-57 Mössbauer spectra of $(\gamma\text{-}Fe_2O_3)_{80}Ag_{20}$ obtained at 295 K (a) and 78 K. (b) The expansion of the velocity scale at 78 K should be noted.

the quadrupole splitting of the SP doublet has increased to $\sim$1.1 mm/s, indicating the presence of the expected electronic distortions at the iron sites. At 78 K there is no obvious indication of the presence of any divalent iron.

Magnetization (M) measurements were performed in a superconducting quantum interference device (SQUID) magnetometer. The temperature dependence of M under zero field cooling (ZFC) and field cooling (FC) indicates superparamagnetism in the $\gamma\text{-}Fe_2O_3$ nanoparticles. The maximum of the ZFC curve and splitting of the ZFC and FC curves indicate[3] a T_b of 40 K, see Fig. 3. An average particle diameter of 9 nm is estimated from the expression $T_b = KV/25k_B$, where the bulk anisotropy constant, K, is 4.7×10^4 erg/cm^3, V is the particle volume, and k_B is the Boltzmann constant.[1,4] This average volume is consistent with TEM and XRD data. In comparing magnetization versus applied field at temperatures above T_b, magnetization in-

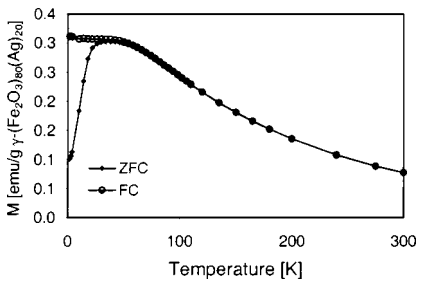

FIG. 3. Zero field cooled (ZFC) and field cooled (FC) magnetization as a function of absolute temperature.

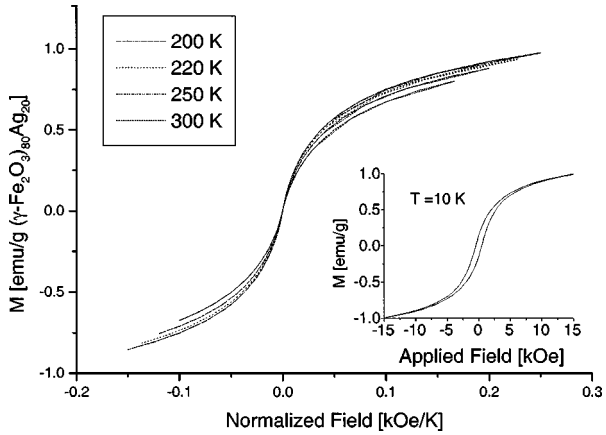

FIG. 4. Normalized magnetization curves of $(\gamma\text{-}Fe_2O_3)_{80}Ag_{20}$ above the blocking temperature. The inset shows the hysteresis at 10 K.

creases without saturation up to an applied field of 30 kOe. This may be due to the wide range of the particle size distribution in the composite as indicated by TEM. The magnetization was plotted as a function of H/T for curves at temperatures above T_b, where H is the applied magnetic field and T is the absolute temperature, see Fig. 4, and it is found that the curves nearly superimpose. Hysteresis measurements made above T_b have zero remanence and coercivity indicating SP behavior. At 10 K, well below T_b, the moments of the nanoparticles are frozen along their anisotropy axes and the magnetization exhibits hysteresis indicating a transition from superparamagnetic to ferrimagnetic behavior, see the inset to Fig. 4. The coercivity is ~400 Oe whereas the coercivity of bulk $\gamma\text{-}Fe_2O_3$ is 250 to 400 Oe.[3]

Magnetoresistance (MR) was determined using a physical properties measurement system (PPMS) modified for resistances greater than 2 MΩ. Defining MR as the percent difference in the resistance at zero field and at an applied field as compared to zero field, it was determined that the nanocomposite exhibits a negative MR of −2.2% at 220 K and 9 T, see Fig. 5. Comparing the MR value of the reverse micelles nanocomposite with ball milled nanocomposites as reported by Tang *et al.*,[2] it should be noted that the negative MR value, of −2.2%, is smaller. The observed negative MR values presented by Tang *et al.* are believed to originate from field dependent electron hopping between Fe^{2+} and Fe^{3+} ions, which depends on the relative orientations of the magnetic moments of the two ions. The same mechanism may be responsible for the magnetotransport in this system. Based on the 295 K Mössbauer spectrum, there is little if any Fe^{2+} present in the reverse micelles nanocomposite. This suggests direct tunneling across $\gamma\text{-}Fe_2O_3$ particles may become a possible transport mechanism although such a claim has yet to be substantiated by experimental results. If this is the case, the MR can then be related to the change of the barrier height of $\gamma\text{-}Fe_2O_3$ due to exchange splitting. The barrier height is the difference between the bottom of the conduction band of $\gamma\text{-}Fe_2O_3$ and the Fermi level of the Ag metal.[5] As a result of the exchange splitting of the conduction band of the ferrimagnetic $\gamma\text{-}Fe_2O_3$, the barrier height for spin-up (spin-down) electrons is reduced (increased), which greatly increases the tunneling probability for spin-up electrons and reduces the probability for spin-down electrons.[6] This leads to the spin-filter effect in which the tunneling current is spin polarized.[7] Thus, the observed negative MR in $(\gamma\text{-}Fe_2O_3)_{80}Ag_{20}$ may be due to the following. The barrier height of $\gamma\text{-}Fe_2O_3$ should not depend strongly on the applied magnetic field as it is determined by the exchange splitting. However, the direction of magnetization of each magnetic nanoparticle is randomly oriented in zero field. Because the so called spin-up and spin-down are relative to the direction of magnetization, the net spin-filter effect is zero because of the random orientation of the magnetic moments of the $\gamma\text{-}Fe_2O_3$ particles. In other words, no reduction in tunneling resistance is expected for any given spin direction. The effect of the applied field is alignment of the magnetic moments of all particles along the field direction reducing the tunneling resistance for electrons whose spins are in the field direction.

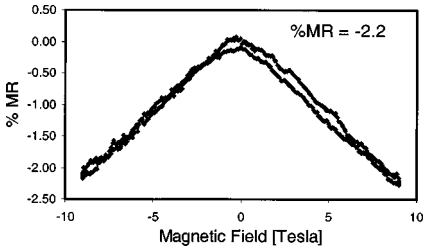

FIG. 5. Magnetoresistance of $(\gamma\text{-}Fe_2O_3)_{80}Ag_{20}$ as a function of applied field at 220 K, the MR= −2.2%.

Transport measurements have been difficult to obtain due to the insulating nature of the nanocomposite. Preliminary voltage versus current curves were obtained at room temperature. The nonlinear shape of the curves may indicate either direct tunneling through the insulator or hopping between iron ions as possible transport mechanisms.

In summary, the negative magnetoresistance of an $(\gamma\text{-}Fe_2O_3)_{80}Ag_{20}$ composite synthesized by reverse micelles has been determined to be ~−2.2% at 220 K and 9 T. There are two possible mechanisms for the observed MR. One is field dependent electron hopping from Fe^{2+} to Fe^{3+}, a hopping which depends on the relative orientations of the magnetic moments of the two ions. The second involves direct tunneling between two Ag particles across the magnetic insulator. When reliable transport data become available the actual mechanism for the observed negative magnetoresistance may be determined.

This research was supported by DARPA (MDA972-97-1-0003) and in part by the U.S. National Science Foundation through a Division of Materials Research Grant No. 95-21739.

[1] R. M. Cornell and U. Schwertmann, *The Iron Oxide Structure, Properties, Reactions, Occurrences and Uses* (VCH, New York, 1996), pp. 30/31, 113–125, 146–170, 368/369, 472/473.
[2] J. Tang, L. Feng, and J. A. Wiemann, Appl. Phys. Lett. **74**, 2522 (1999).
[3] L. Zhang, G. C. Papaefthymiou, and J. Y. Ying, J. Appl. Phys. **81**, 6892 (1997).
[4] B. Martinez, A. Roig, X. Obradors, E. Molins, A. Rouanet, and C. Monty, J. Appl. Phys. **79**, 2580 (1996).
[5] L. Esaki, P. J. Stiles, and S. von Molnar, Phys. Rev. Lett. **19**, 852 (1967).
[6] D. M. Sherman and T. D. Waite, Am. Mineral. **70**, 1262 (1962).
[7] J. S. Moodera, X. Hao, G. A. Gibson, and R. Meservey, Phys. Rev. Lett. **61**, 637 (1988).